

Research on Coupling Vibration Mechanism Based on Contact System

Kepeng HUANG

Xi'an University of Architecture and Technology

Fa-Zhan Wang (✉ wangfz10_1@163.com)

Xi'an University of Architecture and Technology <https://orcid.org/0000-0001-5030-2494>

Ming-Ji Zhao

Xi'an University of Architecture and Technology

Bao-Liang Guo

Xi'an University of Architecture and Technology

Da-Quan Ou

ABB Xin-hui Low-Voltage Switching Co.,Ltd

Original Article

Keywords: Electrical switch, Contact bounce, Electromagnetic force, Collision contact force, Two-degree-of-freedom coupled motion differential equation

Posted Date: August 2nd, 2020

DOI: <https://doi.org/10.21203/rs.3.rs-50694/v1>

License: © ⓘ This work is licensed under a Creative Commons Attribution 4.0 International License.

[Read Full License](#)

Title page

Research on Coupling Vibration Mechanism Based on Contact System

Ke-Peng Huang, born in 1995, study in master candidate at *Xi'an University of Architecture & Technology, China*. He received his bachelor degree from *Xi'an University of Architecture & Technology, China* in 2018. His research interests include electrical switch, vibrating machinery, vibration theory and application.

Tel: +86-15502937890

E-mail: 15502937890@163.com

Fa-Zhan Wang, born in 1966, is currently a professor and a PhD candidate supervisor at *Xi'an University of Architecture & Technology, China*. His main research interests include mechachonics engineering, electrical switch.

E-mail: wangfz10_1@163.com

Ming-Ji Zhao, born in 1996, is currently a master candidate at *Xi'an University of Architecture & Technology, China*.

E-mail: zhao_ming_ji@163.com

Bao-Liang Guo, born in 1966, is currently a professor and a master candidate supervisor at *Xi'an University of Architecture & Technology, China*. His main research interests include vibrating machinery, vibration theory and application.

E-mail: 1063064225@qq.com

Da-Quan Ou, born in 1992, is currently a master candidate at *Xi'an University of Architecture & Technology, Working in ABB Xin-hui Low-Voltage Switchgear Co., Ltd, China*.

E-mail: 2690462086@qq.com

Corresponding author: Fa-Zhan Wang, E-mail: wangfz10_1@163.com

ORIGINAL ARTICLE

Research on Coupling Vibration Mechanism Based on Contact System

HUANG Kepeng¹ • WANG Fazhan¹ • ZHAO Mingji¹ • GUO Baoliang¹ • OU Daquan²

Received June xx, 2020; revised xx xx, 2020; accepted xx xx, 2020

© Chinese Mechanical Engineering Society and Springer-Verlag Berlin Heidelberg 2020

Abstract: Aiming at the problem of vibration and bounce caused by the collision and contact of the moving and static contacts of the electrical switching device during the closing process, based on the comprehensive consideration of the nonlinear electromagnetic force and the collision contact force, the two-degree-of-freedom coupled motion differential equation of the contact system is established, and to solve and experimental analysis. The theoretical and experimental results show that the contact has not separated after the collision, and the iron core has collided, which further intensifies the contact bounce; when the iron core bounces for the second time, it does not affect the bounce of the contact; the contactor is in operation. In this case, the movement of the moving iron core will cause slight jitter of the system. The research results provide a theoretical basis for further control and reduction of contact bounce.

Key words: Electrical switch • Contact bounce • Electromagnetic force • Collision contact force • Two-degree-of-freedom coupled motion differential equation

1 Introduction

The contact system is an important component widely used in electrical switching devices. In fact, it is a kind of nonlinear vibration behavior, in which the collision bounce between the moving and static contacts is an important factor affecting its dynamic characteristics^[1-3]. The small distance separation of the contact parts caused by the collision and bounce can easily lead to the generation of arcs. In severe cases, fusion bonding will occur, which directly affects the electrical contact performance and service life^[4-5]. Therefore, it is an urgent need to analyze the vibration mechanism accurately, grasp the dynamic characteristics change law, and obtain the theoretical method to effectively reduce and suppress the contact bounce, which is an urgent need to improve the electrical life and reliability of electrical components.

✉ Fa-Zhan Wang
wangfz10_1@163.com

¹ Mechanical and Electrical Engineering Xi'an University of Architecture & Technology, Xi'an 710055, China

² Technology R&D Center ABB Xin-hui Low-Voltage Switchgear Co., Ltd, Jiangmen 529000, China

In recent years, domestic and foreign scholars have done a lot of useful work on the analysis of the dynamic process of the contact system. Regarding the establishment of the contact bounce model, JIN P^[6], used the equivalent magnetic circuit model to solve the coupling calculation problem of the magnetic field and mechanical motion generated by the electromagnetic and permanent magnets in the permanent magnet contactor, and deduced the coupling circuit model and the mechanical model Equation of motion. HE K H^[7], analyzed the bouncing of the contact when the contactor is connected, and then obtained the physical process model of the mechanical bounce of the contact, and established the energy balance equation before and after the contact collision. LIN S Y, et al^[8-9], used Cauchy's stress equation to calculate the displacement after considering the collision and deformation. Through the law of conservation of momentum, the control equations of the moving parts of the AC contactor during the bounce process are obtained, and regarding the research on inhibition and reduction of contact bounce. XU Z H, et al^[10-12], proposed the structure of the unsynchronized contact system of the intelligent AC contactor, and studied the zero current breaking control. YANG W Y, et al^[13-17], based on the ANSYS finite element method, simulated the electromagnetic force during the closing process, and considered the influence of the magnetic ring and magnetic leakage. There are three main methods for measuring contact bounce. One is ZHANG D K^[18], designed a measuring device to record the bounce time; the other is that ZHOU L^[19], connected the moving and static contacts into a DC circuit to reflect the bounce of the contactor during the closing process by measuring the voltage change at both ends of the resistance in the circuit; and the last one is CHEN D W^[20], applied high-speed photography technology to set the first open phase and the non-first open phase on the side of the moving contact mark the point, get the contact bouncing by shooting to observe the displacement of the mark.

In summary, scholars at home and abroad have done some useful work on the research of the contact bounce characteristics, but a large amount of work is to analyze the dynamic characteristics of electromagnets through simple

coupled motion equations, circuit equation and magnetic circuit equation, and the vibration mechanism of contact bounce has not been studied^[21]. Therefore, on the basis of the above research, this paper proposes to take the contactor as an example, take the mechanical vibration of the contact system as the entry point, establish a two-degree-of-freedom coupled motion differential equation based on the vibration characteristics, and use high-speed photography technology for experimental verification. It provides a theoretical reference for the optimal design of the contactor.

2 Working principle of AC contactor

The AC contactor is composed of three parts: contact system, electromagnetic system and contact bracket. It is shown in Figure 1.

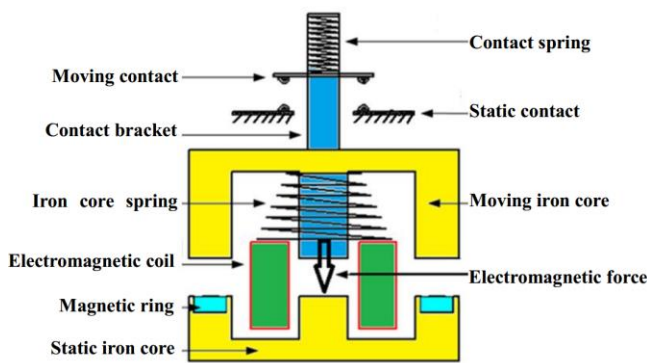


Figure 1 Configuration of the exoskeleton arm system

When the AC contactor is working, first energize the solenoid coil. When the electromagnetic force is greater than the force of the spring, the moving iron core makes the moving contact move downward through the contact bracket. Because the distance between the moving and static contacts is less than that between the moving and static cores, the moving contact will collide and bounce earlier than the moving iron core. At this time, the moving core continues to move downward until the static and moving cores collide, which makes the moving contact bounce again. Due to the collision between the moving and static iron cores, the movement process of the moving contacts that are already bouncing becomes more complicated. Therefore, how to accurately analyze the movement state and the bounce of the moving and static iron cores before and after collision is the key and difficult point in the research on the dynamic characteristics of the contactor.

3 Two-degree-of-freedom coupled motion differential equation

The nonlinearity and discontinuity of the AC contactor on and off make the dynamic characteristics of the AC

contactor system appear abrupt change.

This paper assumes that: (1) The moving parts of the contactor can only move in one direction without displacement or rotation in the other direction; (2) The collision force between contactor parts is caused by local contact deformation, and is based on velocity and collision contact time are used as calculation parameters. Therefore, the piecewise model can be used to establish the piecewise linear vibration differential equation.

3.1 Model establishment

During the operation of AC contactor, it can be equivalent to a two-degree-of-freedom damped forced vibration system, as shown in Figure 2.

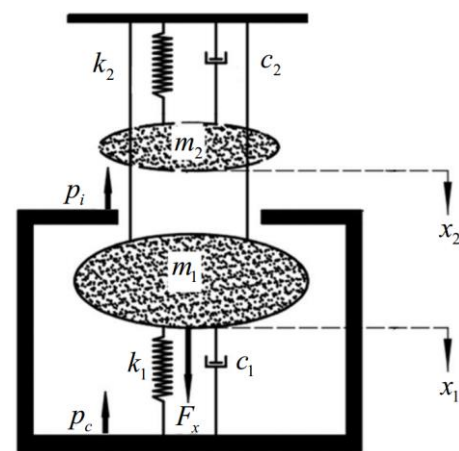


Figure 2 Vibration model of AC contactor system

Where m_1 and m_2 are the mass of the moving iron core and moving contact; x_1 and x_2 are the length of the moving iron core and the displacement of the moving contact; c_1 and c_2 are the equivalent damping of the electromagnetic mechanism and contact system; k_1 and k_2 are the stiffness coefficients of the reaction spring and contact spring; F_x is the electromagnetic force; p_i and p_c are the contact force when the contact and core collide.

The closing motion process of the contactor can be divided into the following three stages: In the first stage, when the moving and static contacts have not yet collided and contacted; in the second stage, when the moving and static contacts have first collided and contacted, the moving and static iron cores have not yet collided, and the collision contact force between the moving and static contacts are considered; in the third stage, when the moving and static iron cores first collide, consider the moving and static iron core collision contact force. The differential equations of motion are:

$$\left. \begin{aligned} m_1 \ddot{x}_1 + c_1 \dot{x}_1 + c_2(\dot{x}_1 - \dot{x}_2) + k_1 x_1 + k_2(x_1 - x_2) &= F_x \\ m_2 \ddot{x}_2 + c_2(\dot{x}_2 - \dot{x}_1) + k_2(x_2 - x_1) &= 0 \end{aligned} \right\}, \quad (1)$$

$$\left. \begin{aligned} m_1 \ddot{x}_1 + c_1 \dot{x}_1 + c_2(\dot{x}_1 - \dot{x}_2) + k_1 x_1 + k_2(x_1 - x_2) &= F_x \\ m_2 \ddot{x}_2 + c_2(\dot{x}_2 - \dot{x}_1) + k_2(x_2 - x_1) &= -P_i \end{aligned} \right\}, \quad (2)$$

$$\left. \begin{aligned} m_1 \ddot{x}_1 + c_1 \dot{x}_1 + c_2(\dot{x}_1 - \dot{x}_2) + k_1 x_1 + k_2(x_1 - x_2) &= F_x - P_c \\ m_2 \ddot{x}_2 + c_2(\dot{x}_2 - \dot{x}_1) + k_2(x_2 - x_1) &= 0 \end{aligned} \right\}, \quad (3)$$

3.2 Electromagnetic force

During the closing process of the AC contactor, the force of the moving contact and the moving iron core is simplified, x_i and x_c are the total stroke of the moving contact and the moving iron core respectively. The result is shown in Figure 3.

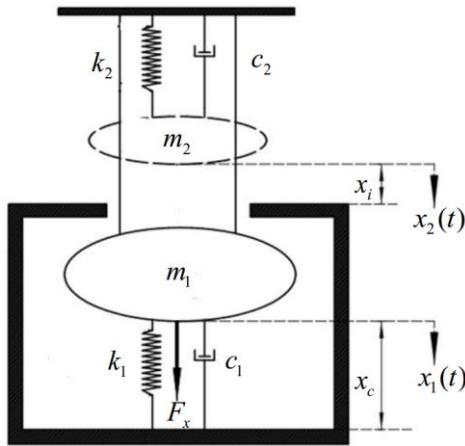


Figure 3 Force model of AC contactor

The closing force process can be divided into two stages: In the first stage, when the moving and static contacts and the moving and static iron cores are not in contact, since the moving contact and the moving iron core are connected by the contact bracket, they move downward together. In the second stage, when the moving and static contacts are in contact and the moving and static iron cores are not in contact, the moving contacts and the moving iron core are separated. At this time, only the moving iron core moves downward. The equation is:

$$\left\{ \begin{aligned} (m_1 + m_2)a + (c_1 + c_2)v + k_1 x_1(t) &= F_x \\ a(t) &= \frac{dv(t)}{dt} \\ v &= \frac{dx_1(t)}{dt} \\ 0 < x_1(t) < x_i \end{aligned} \right. , \quad (4)$$

$$\left\{ \begin{aligned} m_1 a + c_1 v + k_1 x_1(t) + k_2 x_2(t) &= F_x \\ a(t) &= \frac{dv(t)}{dt} \\ v &= \frac{dx_2(t)}{dt} \\ x_i < x_1(t) < x_c \\ 0 < x_2(t) < x_c - x_i \end{aligned} \right. , \quad (5)$$

By combining formula (4) and formula (5), the electromagnetic force of the moving iron core can be solved.

3.3 Contact force

The contact belongs to an elastic body, so the collision will cause periodic bounce during the closing process. The physical process of the contact bounce is shown in Figure 4.

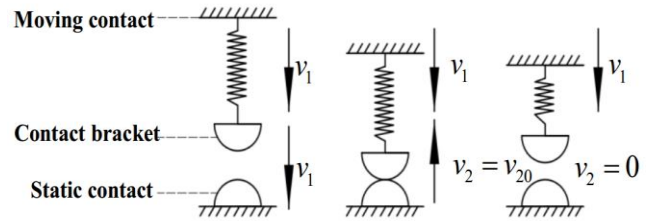


Figure 4 Model of contact bounce

Ignoring the mass of the spring, and m_2 is the mass of the moving contact. It can be seen from Figure4 that the moving contact moves toward the static contact at the velocity of v_1 .

If friction and medium resistance are ignored, the kinetic energy before the collision of the moving contact and the static contact is $1/2m_2v_1^2$. After the contact collision, the kinetic energy of the moving contact is converted into the potential energy of the deformation of the contact surface material (excluding friction). When the elastic deformation recovers, the contact will rebound, making the initial velocity of the moving contact's rebound become v_{20} , and the corresponding kinetic energy is $1/2m_2v_{20}^2$. Then the energy balance equation before and after contact collision is:

$$\frac{1}{2}m_2v_1^2 = \frac{1}{2}m_2v_{20}^2 + K \frac{1}{2}m_2v_1^2, \quad (6)$$

In this paper, the contact recovery coefficient is K .

According to the momentum theorem

$$p_i t_i = m_2 v_2 - m_2 v_1, \quad (7)$$

The contact time of the contact is t_i .

Similarly, the energy balance equation before and after the iron core collision is

$$\frac{1}{2} m_1 v_1^{*2} = \frac{1}{2} m_1 v_{20}^{*2} + K^* \frac{1}{2} m_1 v_1^{*2}, \quad (8)$$

$$p_c t_c = m_1 v_2^* - m_1 v_1^*, \quad (9)$$

The impact time of the iron core is t_c . The velocity of the moving iron core moving along the direction of the static iron core is v_1^* . The initial speed of the reverse jump of the moving iron core is v_m^* . The recovery coefficient of the core material is K^* .

3.4 Two-degree-of-freedom coupled motion differential equation solution

In this paper, ABB A9-30-10 electromagnetic contactor is taken as an example, and parameter values at different stages are given in Table 1

Table 1 Parameter table of AC contactor

Parameter name	Parameter value
$m_1(g)$	200
$m_2(g)$	2
$c_1(N \cdot s / mm)$	30
$c_2(N \cdot s / mm)$	4
$k_1(N / mm)$	0.35
$k_2(N / mm)$	0.25
$x_i(mm)$	4.5
$x_c(mm)$	6
K	0.8
K^*	0.5

Using the MATLAB command ode23 function to solve equations (1), (2 and (3) numerically, and the results are shown in Figure5 and Table 2.

Among them: closing time refers to the time from the beginning of the AC contactor closing to the first contact of the contact; the bounce time refers to the time from the first bounce of the contact to the end of the last bounce; the contact stabilization time refers to the time from The time from the beginning of the contactor to the end of the last bounce of the contact, the same goes for the iron core.

From Figure 5 and Table 2, we can see that the contact closing time corresponds to the first stage of the equation (0ms~23.37ms), and the time from the first bounce of the contact to the first bounce of the core is the second stage of the equation (23.37ms ~23.90ms), the time from the start of

the first bounce of the core to the end of the second bounce of the contact is the third stage of the equation (23.90ms~29.08ms).

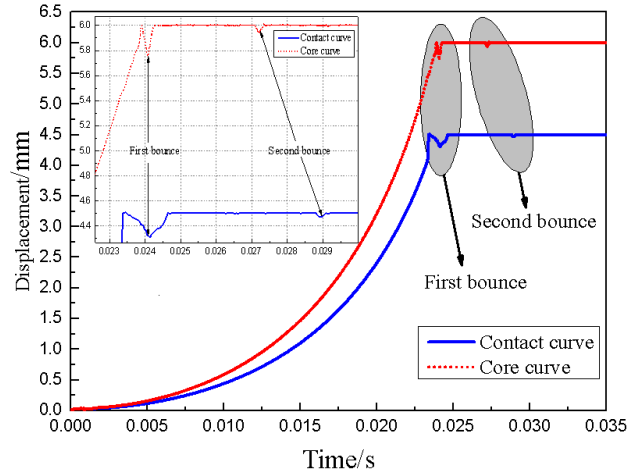


Figure 5 Curve of MATLAB operation result

Table 2 Comparison of results

Category	Moving contact	Moving iron core
Closing time/ms	23.37	23.90
The first bounce(start time)/ms	23.37	23.90
The first bounce(end time)/ms	24.65	24.25
The second bounce(start time)/ms	28.81	27.07
The second bounce(end time)/ms	29.08.	27.35
Total time to bounce(first)/ms	1.28	0.35
Total time to bounce(second)/ms	0.27	0.28
Bounce time/ms	5.71	3.45
Contact stabilization time/ms	29.08	27.35
Maximum bounce amplitude(first)/mm	0.241	0.195
Maximum bounce amplitude(second)/mm	0.049	0.032
Maximum bounce amplitude/mm	0.241	0.195

The first bounce of the contact. It can be seen that the contact bounces earlier than the iron core, but ends after the iron core, and the bounce amplitude of the contact is greater than that of the iron core. This is because the distance between the moving and static contacts is smaller than the distance between the moving and static iron core. The iron core mass is much larger than the contact mass, so the fall cycle is short. Secondly, the contact has not been separated after the collision, and the iron core collided, which further intensified the bounce of the contact and increased its bounce displacement.

The second bounce of the contact. It can be seen that the start and end time of the second bounce of the iron core are earlier than the contact. It can be clearly observed from Figure 5 that when the second bounce of the iron core occurs, the bounce of the contact is not significantly affected. This is because the second bounce amplitude of the iron core is much smaller than the first one, which is consumed by the system itself and not transmitted to the contacts.

It can be seen from that the bounce time, contact stabilization time and maximum bounce amplitude of the contact are larger than the iron core. This is because the contact area of the iron core is larger when it hits, and it is always subjected to electromagnetic force during the bounce process, which further prevents the iron core from bouncing again.

4 Experiment and comparison

In order to get the whole dynamic process of contact bouncing intuitively, this paper adopts high-speed photography technology (EoSens-mini2 system) to take photographic measurement of a group of contacts of ABB's A9-30-10 electromagnetic contactor. Since the bounce time of the contact during the closing process of the AC contactor is very short, generally only 2-6 milliseconds, in order to ensure that the camera can accurately capture the whole process of bounce. Pixels were selected in this paper for shooting, and the shooting speed was 43540 frames per second. Figure 6 (a) and (b) are the layout of the contactor prototype and experimental equipment.

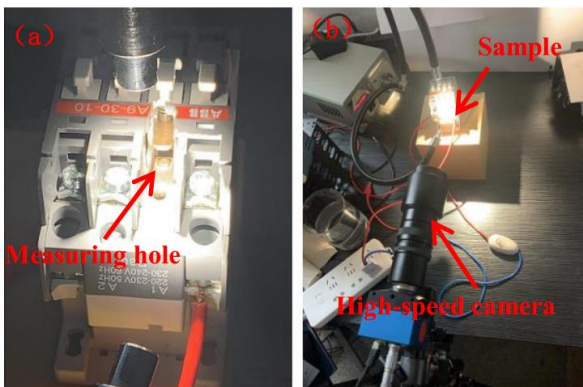


Figure 6 Shooting layout

The specific steps are as follows: first, a measuring hole is opened on one side of the contactor directly facing the position of the contact group; then, the high-speed camera is aimed at the contact head position and focused; finally, the moving contact head position is marked and monitored in the high-speed camera; meanwhile, the shooting parameters of the camera are adjusted and the camera is started for shooting.

Figure 7 (a), (b) and (c) are screenshots of the moving and static contacts that have not yet collided, the moving and static contacts have collided, and the moving and static iron cores collided during the contact bounce process. That is, it corresponds to the first stage, the second stage and the third stage in the closing process of the contactor.

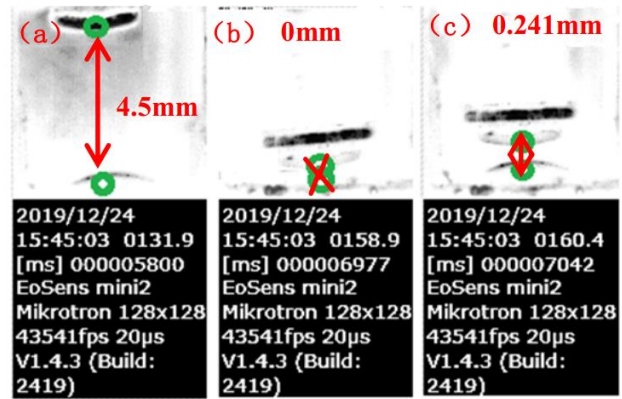


Figure 7 Contact of bounce process

The processing program is applied to MATLAB software to process the above-mentioned collected images, mainly divided into the following steps (as shown in Figure 8).

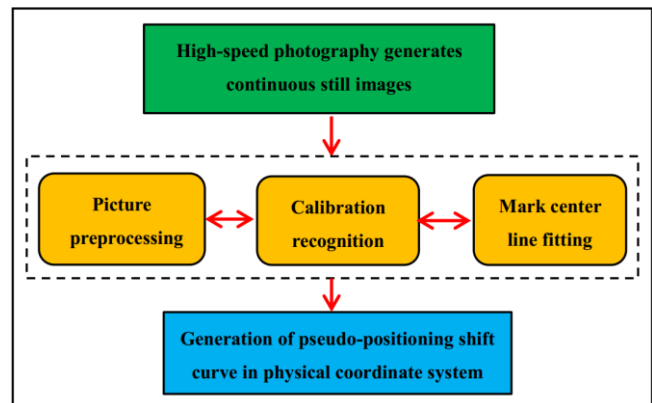


Figure 8 Data processing Flowchart

- (1) Image preprocessing: the collected image is processed by noise removal and enhancement to extract the geometric information of image feature points.
- (2) Calibration and identification: according to the black and white pixel features in the image, the moving and static contact components are highlighted, as shown in Figure 6 and then the program is used to identify the marked points, and extract the image coordinate system after the value of the two images.
- (3) Line fitting of marked center: image coordinate values are extracted from the value of the two images, and line fitting of marked center circle diameter is performed on the coordinates of marked points by using least square method.
- (4) Calibration of object coordinate system and generation of displacement curve: the solution of the center circle diameter of the mark is transferred to the linear relationship between the two coordinate systems, and then the processing results of each picture are arranged according to the collected time series to obtain the experimental curve of the displacement of the mark point. The results are shown in Figure 9.

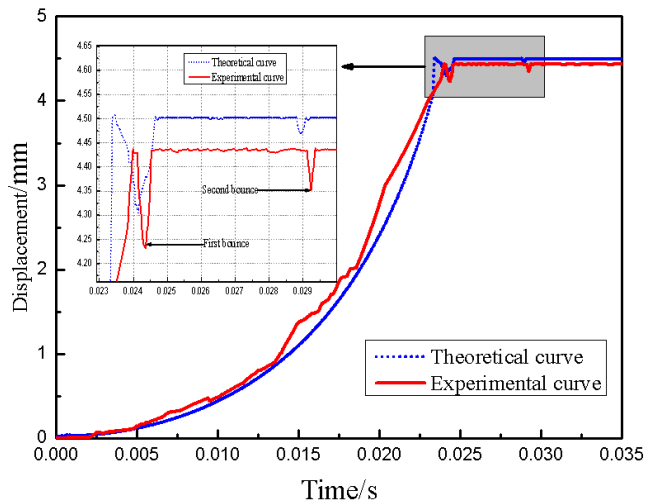


Figure 9 Distributed control system of the master arm

It can be seen from Figure 9 that the overall trend of the experimental curve and the theoretical curve is the same. The contacts have two obvious bounces, but the contacts in the first stage, and the experimental curve is not smooth. This is because the contactor is in actual operation. , The movement of the moving iron core will cause a slight jitter of the contactor system, so the experimental curve is not smooth. Secondly, the experimental curve and the theoretical curve do not fit perfectly in the second and third stages. This is caused by the data measurement error in the process of measuring the model parameters in the establishment of the contactor model. This error will not affect the equation solution. So the result is negligible.

Table 3 Comparison between theory and experiment

Category	Theory	Experiment	Error /%
The first bounce(start time)/ms	23.37	23.67	1.28
The first bounce(end time)/ms	24.65	24.52	0.53
The second bounce(start time)/ms	28.81	29.09	0.97
The second bounce(end time)/ms	29.08	29.34	0.89
Closing time/ms	23.37	23.67	1.28
Bounce time/ms	5.71	5.67	0.70
Contact stabilization time/ms	29.08	29.34	0.89
Maximum bounce amplitude/mm	0.241	0.252	4.56

The specific numerical values of experimental results and theoretical results are shown in Table 3. It can be seen from Table 3 that the start time and end time of the two bounces, closing time, bounce time, contact stabilization time, and maximum bounce amplitude error of the experimental and theoretical contacts are all within 5%, indicating that the experimental and theoretical results are highly consistent. The accuracy and reliability of the theory are verified.

5 Conclusions

(1) From the perspective of vibration, considering the nonlinear electromagnetic force and collision contact

force, a two-degree-of-freedom coupled motion differential equation of the contact system is established.

- (2) The first bounce of the contact starts earlier than the iron core and ends later than the iron core, and the bounce amplitude is greater than that of the iron core. The contact has not been separated after the collision contact, and the iron core collided, which further intensified the contact bounce. The start and end time of the second bounce of the contact is later than that of the iron core. When the second bounce of the iron core occurs, it does not affect the bounce of the contact.
- (3) The bounce time, contact stabilization time and maximum bounce amplitude of the contact are all greater than the iron core. In addition, during the operation of the contactor, the movement of the moving iron core will cause a slight vibration of the contactor system.

6 Declaration

Acknowledgements

The authors sincerely thanks to ABB Xin-hui Low-Voltage Switch Co., Ltd. provided a series of contactor samples and key components for this research, Xi'an Jiao tong University Energy and Dynamics provided a high-speed photographic laboratory platform for this research, and professor Fa-Zhan Wang of Xi'an University of Architecture & Technology for his critical discussion and reading during manuscript preparation.

Funding

Supported by Natural Science Foundation of Shanxi Province(Grant No. 2011J2009).

Availability of data and materials

The datasets supporting the conclusions of this article are included within the article.

Authors' contributions

The author' contributions are as follows: Fa-Zhan Wang and Bao-Liang Guo were in charge of the whole trial; Ke-Peng Huang wrote the manuscript; Ming-Ji Zhao and Da-Quan Ou assisted with sampling and laboratory analyses.

Competing interests

The authors declare no competing financial interests.

Consent for publication

Agree.

Ethics approval and consent to participate

Not applicable

References

- [1] L Shu, L Wu, G Wu, et al. A fully coupled frame-work of predicting the dynamic characteristics of permanent magnet contactor [J]. *IEEE Transactions on Magnetics*, 2016;52(8):1.
- [2] V BIAGINI, P BOLOGNESI, G MECHLER, et al. Multi-domain mechatronic approach for the design of a vacuum contactor actuation drive [C] // *Xxii International Conference on Electrical Machines IEEE*, 2016:1126—1131.
- [3] G S Chen, Z Ca. Design and optimization of energy-saving wind power grid-connected contactor based on Nano two-phase composite magnetic materials [C] // *2017 4th International Conference on Electric Power Equipment Switching Technology*, 2017:209—212.
- [4] W B Ren, L Cui, G F Zhai. Contact Vibration characteristic of electromagnetic relay[J]. *IEICE transactions on electronics*, 2006,E89-C(8):1177-1181.
- [5] B V KLYMENKO, M G PANTEYAT. Electromagnetic actuators for medium voltage vacuum switching devices: classification design controlling [C] // *International Symposium on Electromagnetic Fields in Mechatronics, Electrical and Electronic Engineering*. 2017:1-2.
- [6] P Jin, H Y Lin, S H Fang, et al. A Rapid Magnetic Analysis and Dynamic Prediction Model for Permanent Magnet Contactor (English) [J]. *Proceedings of the Chinese Society for Electrical Engineering*. 2010:16-21. (in Chinese)
- [7] K H He, M Z Rong, Y Wu, et al. Analysis of electromagnetic characteristics for three gaps permanent magnet contactor[J]. *Low Voltage Apparatus*, 2012,(13):6-10. (in Chinese)
- [8] S Y Lin, Z H Xu. Simulations and numerical analysis on 3d dynamic process of alternating current contactors[J]. *Proceedings of the CSEE*, 2014(18):2967-2975. (in Chinese)
- [9] S Y Lin, Z H Xu. Performance characteristics of ac contactor during voltage sag[J]. *Proceedings of the CSEE*, 2011,31(24):131-137. (in Chinese)
- [10] Y Wang, Z H Xu. RBR control strategy for the closing process of intelligent electromagnetic contactors[J]. *Proceedings of the CSEE*, 2019,39(15):4568-4578. (in Chinese)
- [11] J X Wu, Z H Xu. A model-free adaptive control strategy for actuation of electromagnetic contactors[J]. *Proceedings of the CSEE*, 2020,40(5):1663-1672. (in Chinese)
- [12] X Y He, Z H Xu. Virtual prototyping technology of ac contactor[J]. *Transactions of China Electro technical Society*, 2016,31(14):148-155. (in Chinese)
- [13] L X Liu, W Y Yang, R Wang. Overview on modeling method and experimental research of contact spring bounce for electromagnetic relays[J]. *Electrical and Energy Management Technology*, 2017,(9):1-8,29. (in Chinese)
- [14] W Y Yang, L X Liu, Y Liu, et al. Establishing of contactor dynamic model considering collision bounce and analysis of influencing factors of bounce characteristics[J]. *Transactions of China Electro technical Society*, 2019,34(9):1900-1911. (in Chinese)
- [15] W Y Yang, L X Liu, N Jia, et al. Establishing of contactor dynamic model considering collision bounce and analysis of influencing factors of bounce characteristics[J]. *Low Voltage Apparatus*, 2017,(16):83-88. (in Chinese)
- [16] W Y Yang, S Shao, J Zhou, et al. Vibration characteristic simulation study of high power contactor based on ANSYS[J]. *Electrical and Energy Management Technology*, 2018(04):25-28. (in Chinese)
- [17] W Y Yang, L X Liu, G F Zhai. The bounce characteristics of contactors for new energy under the influence of thermal field[J]. *Transactions of China Electro Technical Society*, 2019,34(22):4687-4698. (in Chinese)
- [18] D K Zhang, D Xu. Automatic test equipment of case circuit breaker contact stagger time[J]. *Low Voltage Apparatus*, 2010,(17):57-59. (in Chinese)
- [19] L Zhou, G C Wu, W B Xie. The dynamic testing and analysis on contactors based on laser probing of displacement[J]. *Journal of Wenzhou University(Natural Sciences)* 2013,34(3):32-37. (in Chinese)
- [20] D W Chen, P M Zhang. High-speed camera-based intelligent AC contactor dynamic testing and analysis techniques[J]. *Chinese journal of scientific instrument*, 2010,31(4):878-884. (in Chinese)
- [21] Y F Li, F Z Wang, Y K Wang, et al. Bumping behavior simulation and influencing factors analysis of contact system in contactor[J]. *Mechanical Science and Technology for Aerospace Engineering*, 1003-8728. 2020,0016:1-8. (in Chinese)

Biographical notes

Ke-Peng Huang, born in 1995, study in master candidate at *Xi'an University of Architecture & Technology, China*. He received his bachelor degree from *Xi'an University of Architecture & Technology, China* in 2018. His research interests include electrical switch, vibrating machinery, vibration theory and application.

Tel: +86-15502937890

E-mail: 15502937890@163.com

Fa-Zhan Wang, born in 1966, is currently a professor and a PhD candidate supervisor at *Xi'an University of Architecture & Technology, China*. His main research interests include mechatronics engineering, electrical switch.

E-mail: wangfz10_1@163.com

Ming-Ji Zhao, born in 1996, is currently a master candidate at *Xi'an University of Architecture & Technology, China*.

E-mail: zhao ming ji@163.com

Bao-Liang Guo, born in 1966, is currently a professor and a master candidate supervisor at *Xi'an University of Architecture & Technology, China*. His main research interests include vibrating machinery, vibration theory and application.

E-mail: 1063064225@qq.com

Da-Quan Ou, born in 1992, is currently a master candidate at *Xi'an University of Architecture & Technology, Working in ABB Xin-hui Low-Voltage Switchgear Co., Ltd, China*.

E-mail: 2690462086@qq.com

Appendix

Figures

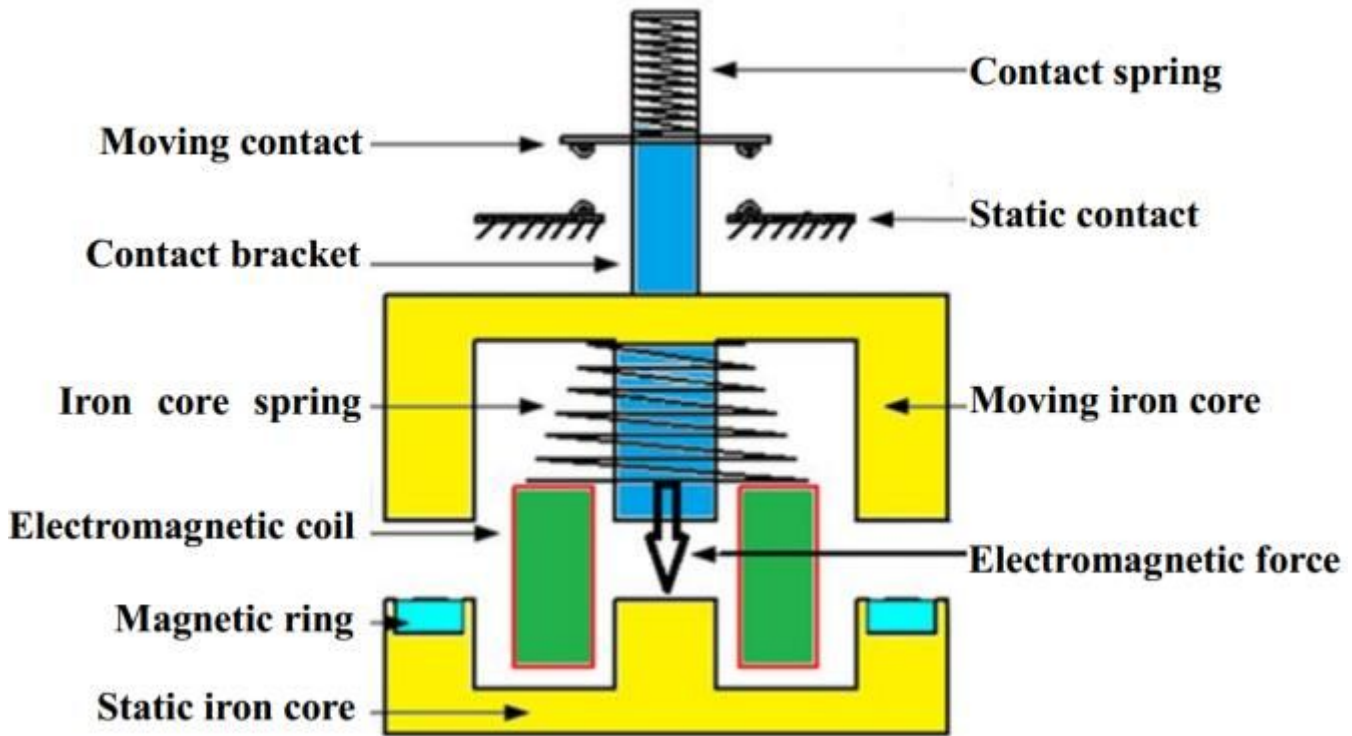


Figure 1

Configuration of the exoskeleton arm system

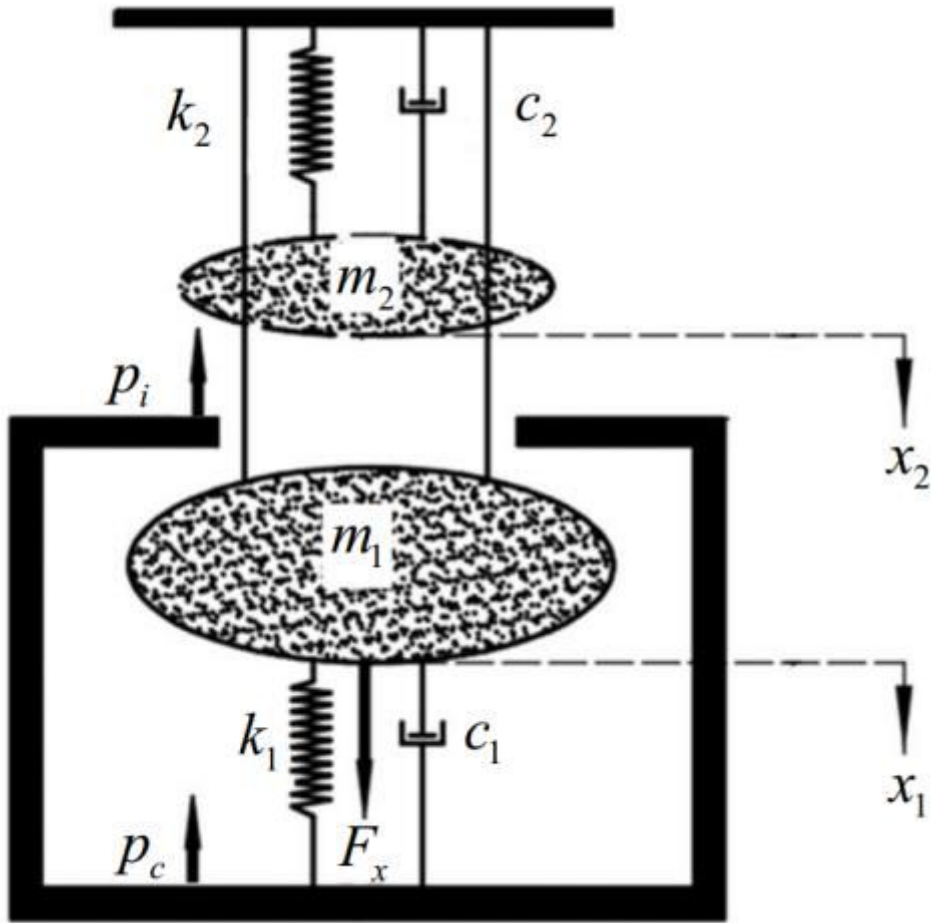


Figure 2

Vibration model of AC contactor system

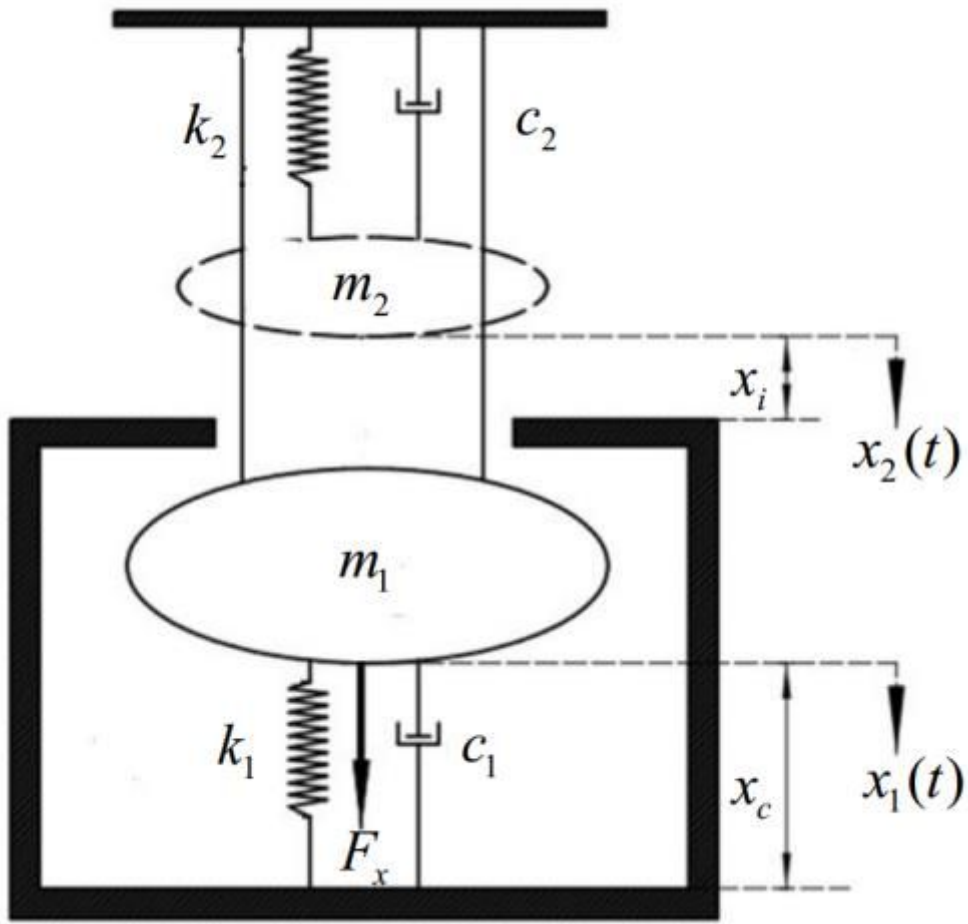


Figure 3

Force model of AC contactor

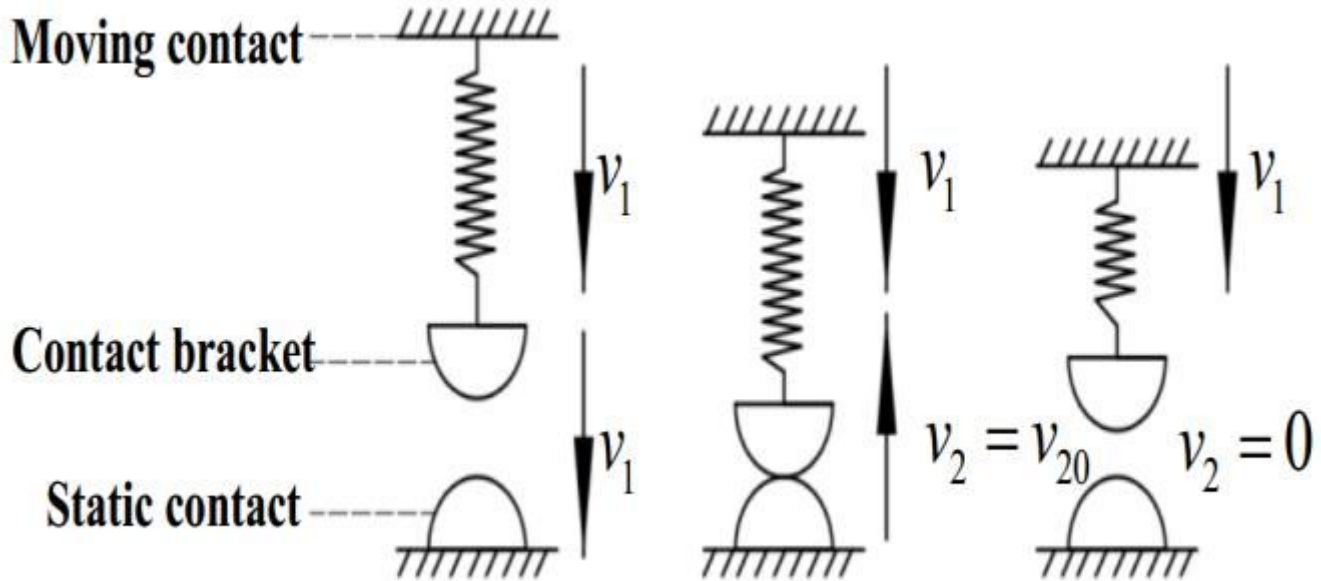


Figure 4

Model of contact bounce

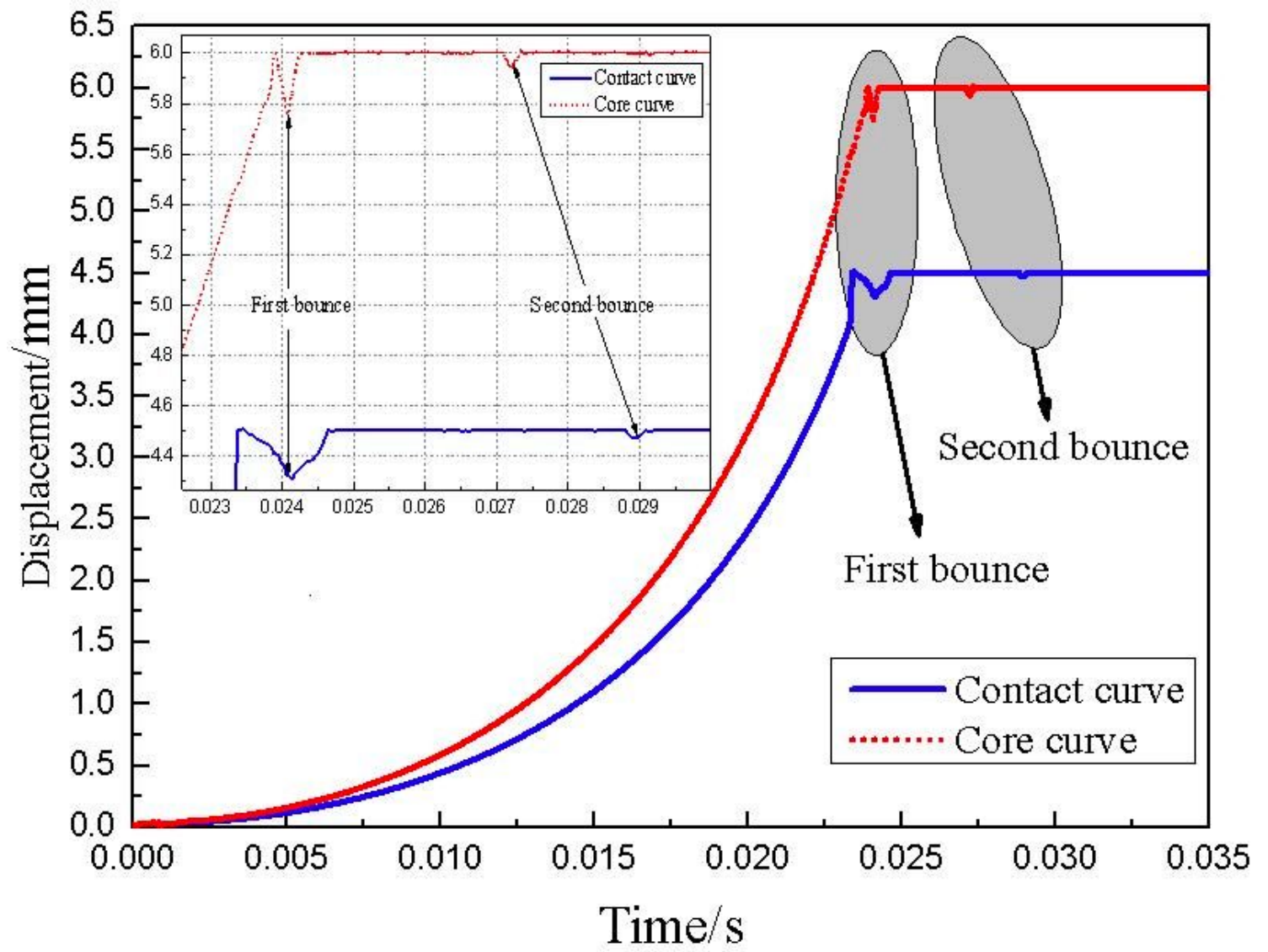


Figure 5

Curve of MATLAB operation result



Figure 6

Shooting layout

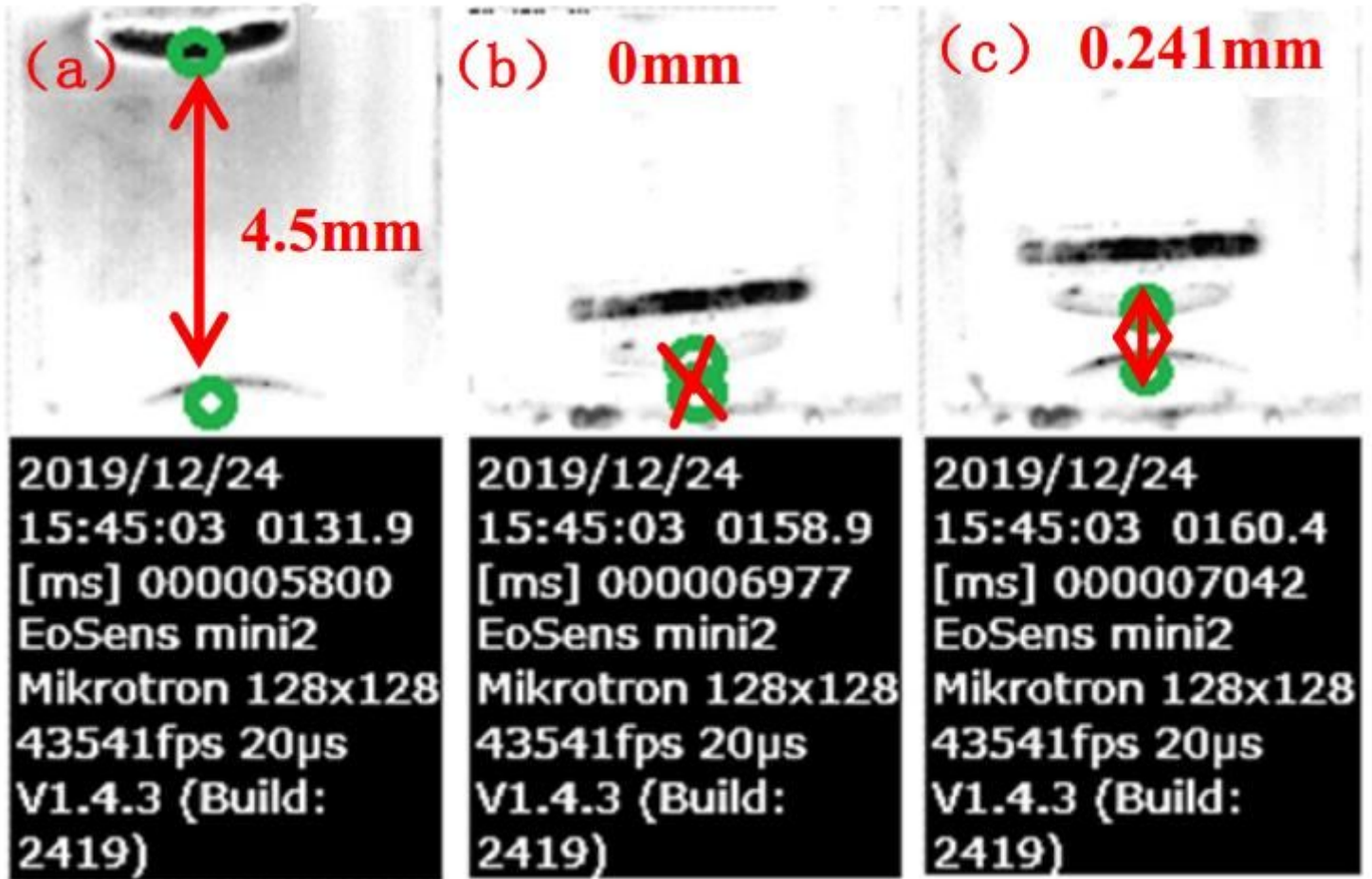


Figure 7

Contact of bounce process

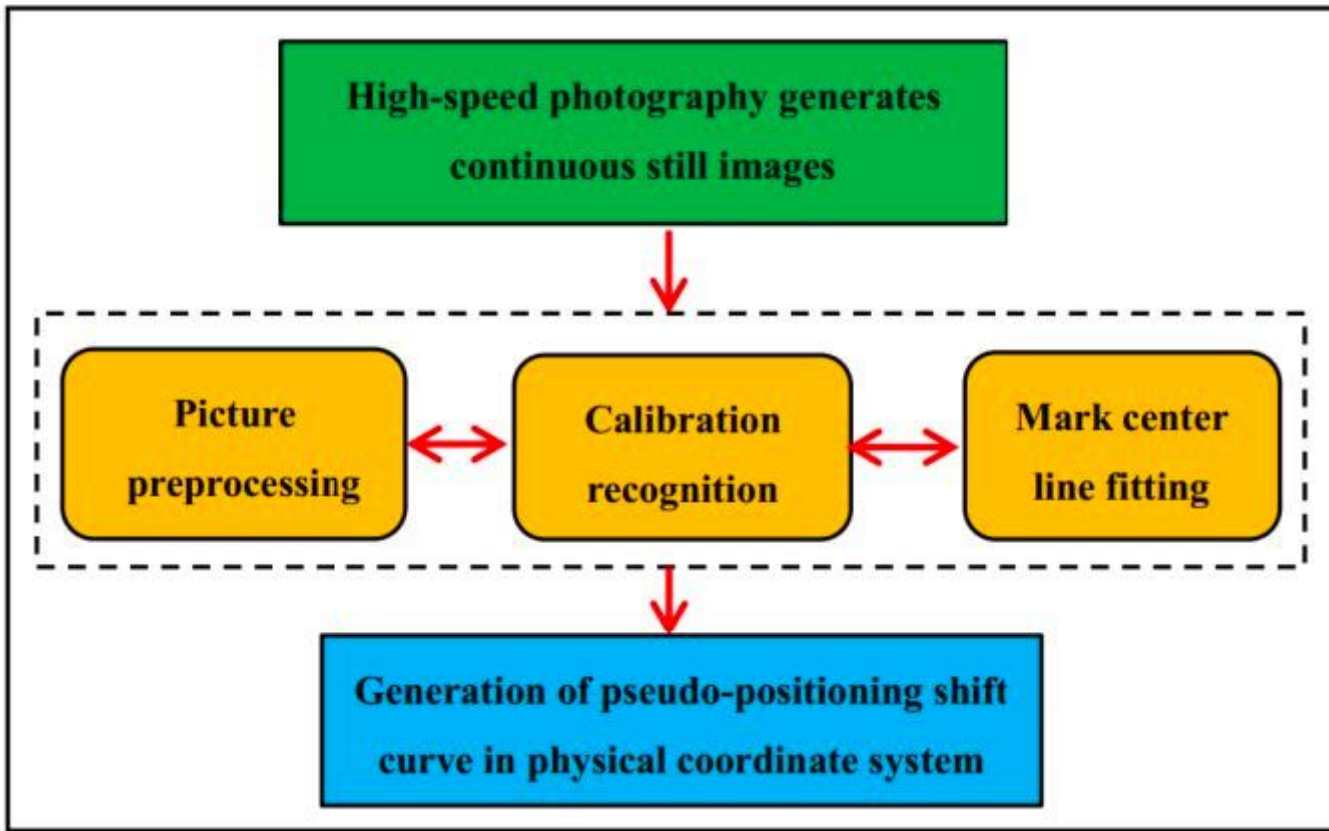


Figure 8

Data processing Flowchart

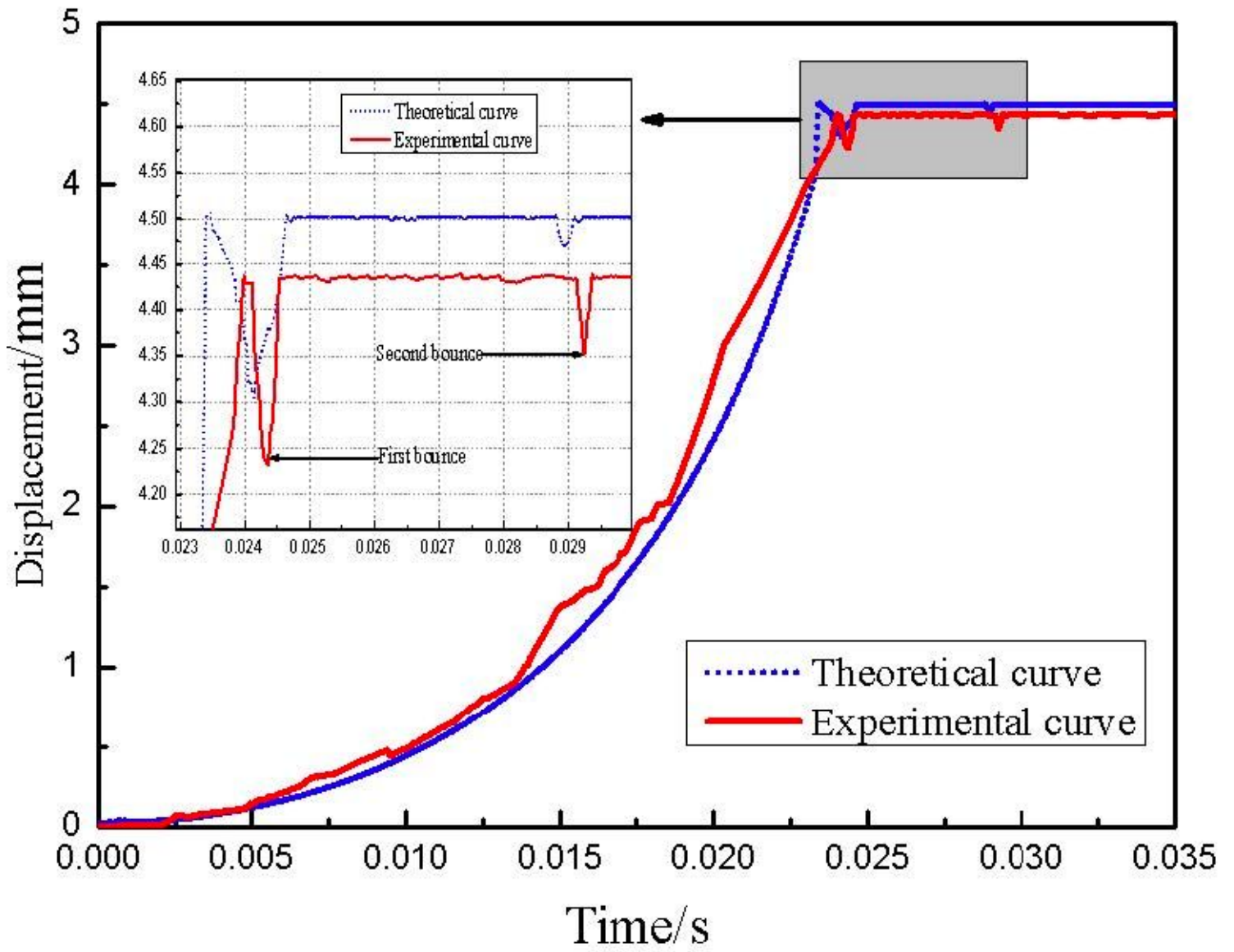


Figure 9

Distributed control system of the master arm